Sigurd Johannes Gaut

Stress Corrosion Cracking of Carbon Steel in Amine Solution

Master's thesis in Materials Science and Engineering
Supervisor: Hilde Lea Lein
July 2019

◼ NTNU
Norwegian University of
Science and Technology

Sigurd Johannes Gaut

Stress Corrosion Cracking of Carbon Steel in Amine Solution

Master's thesis in Materials Science and Engineering
Supervisor: Hilde Lea Lein
July 2019

Norwegian University of Science and Technology
Faculty of Natural Sciences
Department of Materials Science and Engineering

NTNU
Norwegian University of
Science and Technology

Abstract

In this paper, the possibility of Stress Corrosion Cracking or other brittle fracture mechanisms of an S235JR steel in 30% monoethanolamine is examined. Tensile tests at strain rate $10 \times 10^{-6}\,\mathrm{s}^{-1}$ with two samples each were carried out in order to examine the stress-strain behavior in the environment. The experiments were carried out at $60\,°\mathrm{C}$, and atmospheric control was used to keep an atmosphere of 80% N_2 10% CO_2, and 10% O_2 for most cases. Impressed potential cathodic protection was used in hopes of provoking hydrogen induced cracking. Two of the tests used an atmosphere containing H_2S. A few tests were also done for a comparable mixture of amines.None of the samples underwent brittle fracture indicating neither stress corrosion cracking nor hydrogen induced cracking occurred.

Contents

1 Background

Due to rising concerns about global warming, reducing emission of greenhouse gases such as CO_2 is a major concern for traditional industries. One typical method of CO_2 capture from exhaust fumes is a two-column alkanolamine (hereafter "amine") based system. In one column, the amines bind CO_2 from the exhaust fumes. In the second column, higher temperature forces the absorption reaction to reverse, permitting capture of the CO_2 and reuse of the amine solution. Due to the corrosive environments inside the columns, these are usually made from high-cost stainless steels. To save costs, it would be of great interest if one could use a regular carbon steel for the less aggressive environment of the colder column.
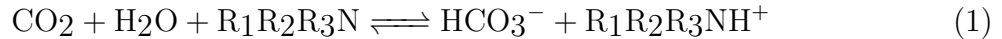
This gives rise to the aim of this work: is carbon steel susceptible to stress corrosion cracking in the relevant amine solutions at $60\,°C$?

2 Introduction

The precise definition of Stress Corrosion Cracking (SCC) varies slightly between sources, but is generally a term given to failure due to cracks formed by synergistic effects of a corrosive environment and applied or residual mechanical stress[1]. Thus, for SCC to occur, three factors must be simultaneously present: A susceptible material, a tensile stress, and a corrosive environment. Typically, SCC does not occur if there is a significant general corrosion rate, but is prevalent in environments that result in film formation on the metal surface. As a result, normally passivating environments such as that created by an aqueous solution of amines are of particular concern for carbon steels[2].

Removal of CO_2 and H_2S from natural gas using amines has been a known process since the 1930s[3]. The same process can be applied to cleansing of exhaust gases from power plants and factories, so-called post combustion capture (PCC). This has increasing relevance in the modern day, as more than three quarters of all greenhouse gas emission is CO_2, most of it from power plants fueled by fossil fuels. While PCC-processes have been shown to be effective on large-scale pilot projects, wide-spread use has as of 2014 not been achieved. This is due to high cost of operation compared to penalties for CO_2 emission, and high energy consumption of the process itself[4].

PCC and gas sweetening facilities that utilize amines work due to the reaction of the basic amine with the acidic CO_2 to form bicarbonate or amine carbamate, along with a protonated amine. The relevant reactions are

$$CO_2 + H_2O + R_1R_2R_3N \rightleftharpoons HCO_3^- + R_1R_2R_3NH^+ \tag{1}$$

$$CO_2 + 2\,R_1R_2NH \rightleftharpoons R_1R_2NCOO^- + R_1R_2NH_2^+ \tag{2}$$

Where R_n indicates either an alkyl group or a hydrogen atom. The forward reaction in both equilibria is exothermic, which means the solution loaded with CO_2 releases it when it is heated. Reaction (2) is faster than Reaction (1), and thus responsible for most of the absorption, but it cannot occur for teritary amines[5]. Previous research shows that primary amines such as Monoethanolamine (MEA) result in more corrosion issues than secondary or tertiary amines when loaded with CO_2, though they are better absorbers of CO_2. Due to this higher effect, MEA represents the benchmark technology for amine-based PCC[3], [6], [7].

Despite SCC being a known issue in MEA installations, the mechanisms are, as is typical of SCC, not well known. A common issue lies in determining a failure as due to SCC when a more accurate analysis shows the failure occurred due to Hydrogen Induced Cracking (HIC). The phenomena result in similar failures, and often in similar systems, but HIC has a clear and definite origin: diffusion of atomic or molecular hydrogen into the metal either forcing crack growth or embritteling the metal. HIC fractures also show much less corrosion products on the fracture surface, whereas SCC features corrosion within the initiating cracks, resulting in a more corroded fracture[2].

This work seeks to examine the failure mechanisms of an austenitic carbon steel, S235JR according to EN 10025-2[8], [9], in amine environments. To this end, tensile testing at strain rate $10^{-6}s^{-1}$ was carried out on samples submerged in solutions of 30% MEA with atmosphere and temperature control. A few tests were also carried out in an experimental mixture of amines developed for carbon capture by Aker BP. This mixture
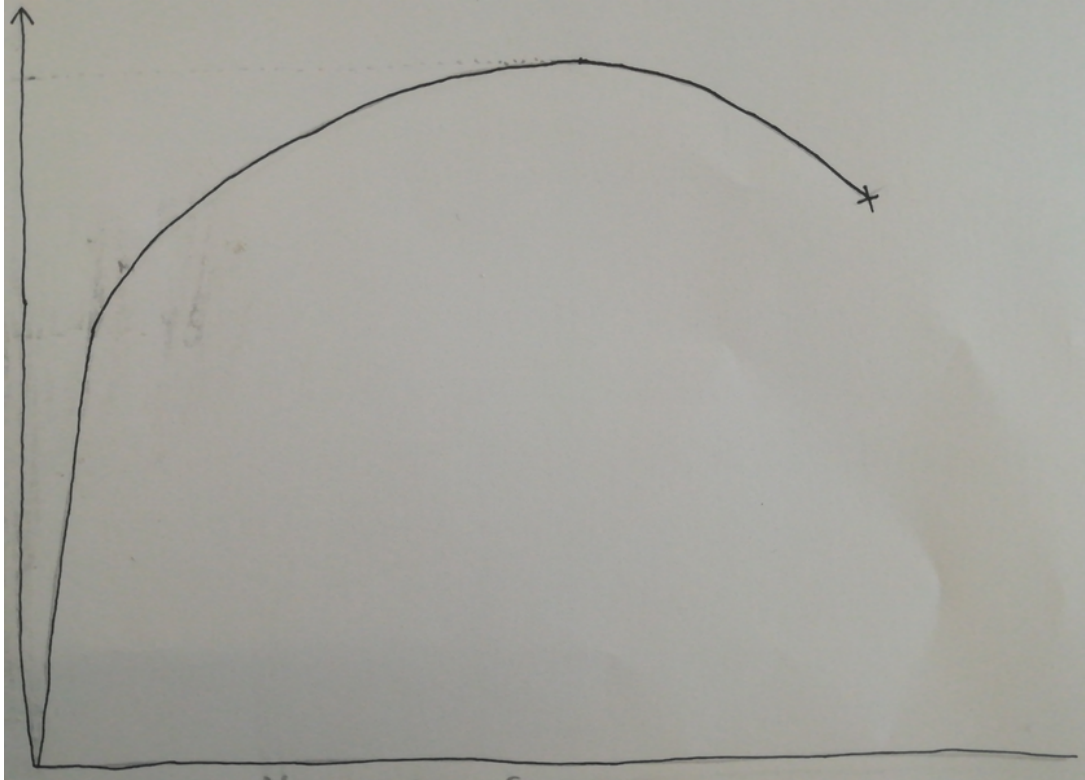
Figure 1: Sketch of nominal Stress-Strain curve for a ductile material. Stress is plotted on the y-axis, strain on the x-axis.

has been labeled "CCX2". Attempts were made to induce HIC by means of impressed potential cathodic protection, as well as tests simulating actual operating conditions using H_2S and CO_2. Tests were also carried out on samples with an included weld, examining whether the weld or heat affected zone is more susceptible to SCC or HIC mechanisms.

When conducting the tensile tests, the recorded data is output as applied force against elapsed time, or equivalently the stroke of the loading unit. Knowing the initial length and thickness of each sample, this can be converted to a stress-strain curve which illustrates the behavior of the material. A typical curve for a ductile material is illustrated in Figure 1. This shows a linear elastic region, followed by a region of plastic deformation where movement of dislocations in the material result in permanent deformation of the material. The point where the material begins to undergo plastic deformation is known as the Yield Strength (YS), and the maximum on the stress-strain curve is known as the Ultimate Tensile Strength (UTS). The UTS is the stress at which fracture will occur without fail if the load is maintained. Beyond the UTS, the material will begin to experience necking, a narrowing of a small segment of the sample, in which all subsequent strain occurs[10].

During these tests, two potential deviations from the general curve are expected, illustrated separately in Figure 2. The first is a brittle fracture, where instead of extensive plastic deformation, and in particular necking, the stress increases until fracture occurs after relatively little deformation. This is seen in Figure 2 a). The second is the yield point phenomenon, or Lüders plateau shown in Figure 2 b). This plateau occurs as a result of a process where interstitial particles "pin" dislocations in place until a higher yield point is reached, seen as a small maximum ahead of the plateau in the sketch.

The plateau itself shows a region of propagating dislocations, but not to such an extent that the material experiences strain hardening[11]. This effect is common in steels like the S235JR being studied. Once dislocation density reaches the point where hardening occurs, the curve rises as seen in the general case.
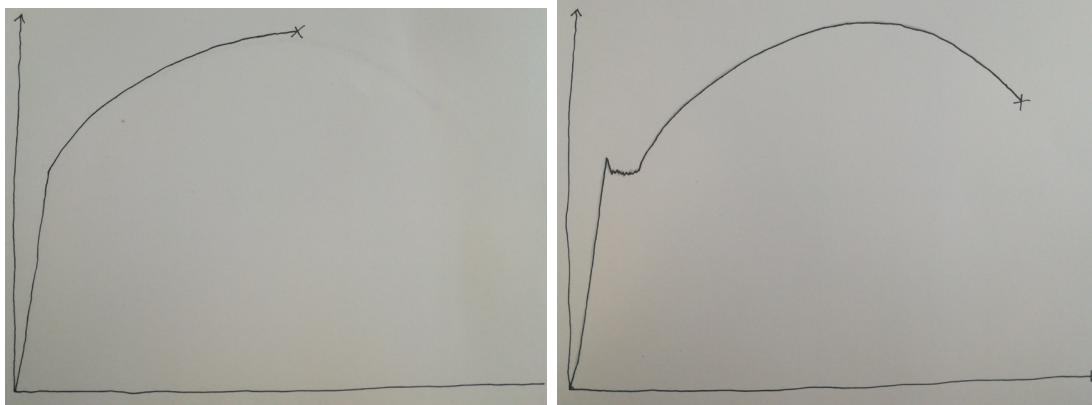
(a) Brittle Fracture   (b) Lüders plateau

Figure 2: Sketches of stress-strain curves for a brittle material, and one displaying the Lüders plateau.

4

3 Equipment and Procedure

3.1 Materials and equipment

The materials used in the experiments in this project are summarized in Table 1.

Table 1: Materials and chemicals used in Slow Strain Rate tensile tests.

Carbon Steel	S235JR
Monoethanolamine (MEA)	Mixed to 30 wt% in water
"CCX2"	Mixture of amines with properties comparable to MEA
gas mixtures	I: pure N_2
	II: 80% N_2 10% CO_2, 10% O_2
	III: 103 ppm H_2S, 10.1% CO_2, rest N_2
	IV: 7.30% H_2S, rest CO_2
	V: 4.83% H_2S, rest CO_2
NaOH	Mixed to 10 mol% in water

The S235JR steel is the material under examination; the aim of the work is to determine whether it may undergo stress corrosion cracking in the MEA or "CCX2" environment. Properties of S235JR from the literature are displayed in Table 2. The gas mixtures were used to simulate possible operating conditions.

Table 2: Chemical composition and mechanical strength of S235JR.[9][8]

C max	Mn max	P max	S max	N max	Cu max	YS	UTS
0.17%	1.40%	0.040%	0.040%	0.012%	0.55%	235 MPa	360-510 MPa

The main piece of equipment utilized for the experiments was an SSRT autoclave from the finnish company Cormet fitted with two loading units, pictured in Figure 3. This enabled running two parallel samples at a constant strain rate, while submerged in the test solution at the same time as both the temperature and the atmosphere were strictly controlled. An external temperature control was used, initially a simple device which turned on or off depending on the temperature registered inside the autoclave. Thi was replaced with a more accurate PID controller starting with test 7. For the tests run with H_2S, an external barometer was used to control the pressure from the gas flask against the pressure in the autoclave. A potentiostat was used along with the Cormet's included Ag|AgCl reference electrode and a Pt counter electrode to produce an impressed potential in some of the experiments.

3.2 Sample preparation

Samples for tensile testing were machined from the S235JR steel material. Each sample was constructed with a tensile region approximately 30 mm long, and approximately 3.15 mm wide. Before use, the samples were polished with sandpaper along their length to remove orthogonal surface cracks potentially left over from the machining. This polishing was done by hand with successively finer sandpaper, first 50p, then 120p, 320p, and
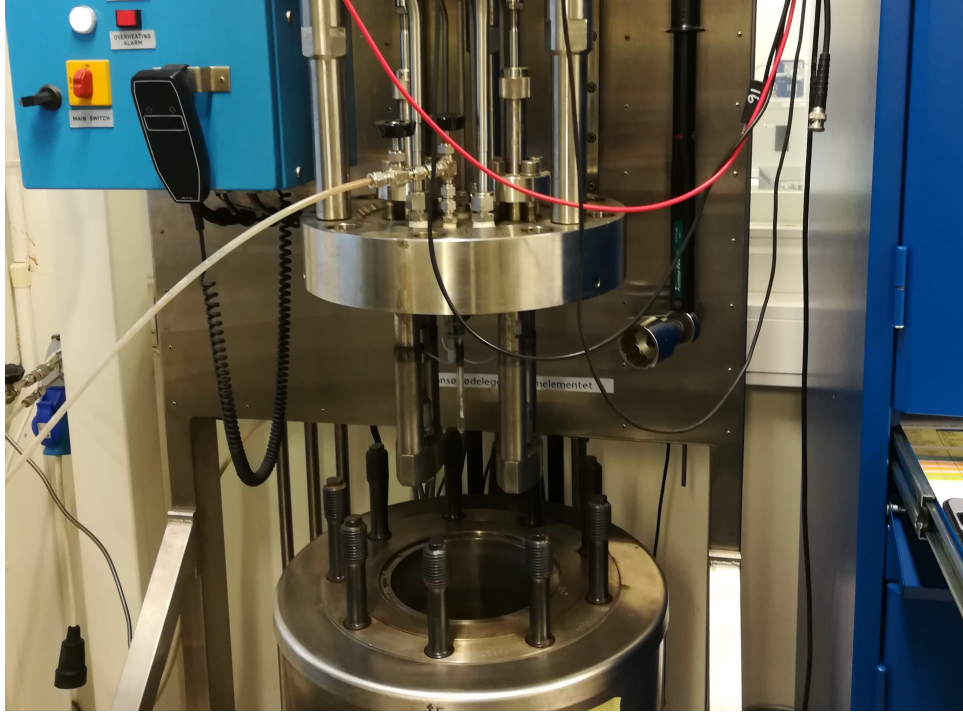
Figure 3: Cormet SSRT autoclave

finally 500p. The exact thickness at each end of each sample after polishing was measured using digital calipers. A full summary of each sample used in the tests is given in Table 4 in the appendix. A sample is imaged in Figure 4. Half of the samples were made to include an overmatch weld, with higher yield strength than the base material. The weld was situated in the middle of each sample, and is imaged as it appeared in the plate material in Figure 5. In order to determine the amount of weld material in the samples, an unused sample was anodized at an impressed potential 1050 mV vs. Ag|AgCl. The weld was then measured using a digital caliper to be between 7.73 mm and 10.31 mm. For two of the tests with impressed potential cathodic protection, the samples were held at the protection potential for an extended time prior to the start of the test. This was done to ensure maximum possible absorption of hydrogen in the steel. Due to restrictions on use of the Cormet rig, the preloading was done in a separate cell. The preloading cell used a Pt wire as counter electrode, an Ag|AgCl reference electrode, and the S235JR samples to be loaded as the working electrode. The electrolyte was 4% NaCl in distilled H_2O. Two welded samples were held at -1050 mV vs. Ag|AgCl for 8 days prior to testing, while two homogeneous samples were held at the same potential a further 3 days for a total of 11 days.

3.3   Experimental procedure

Each stress test was run with two samples in parallel in the Cormet rig, as seen in Figure 7. In each instance, the samples had received the exact same preparation, and were securely fastened. Both samples were put under about 180 N force, and attempted moved laterally

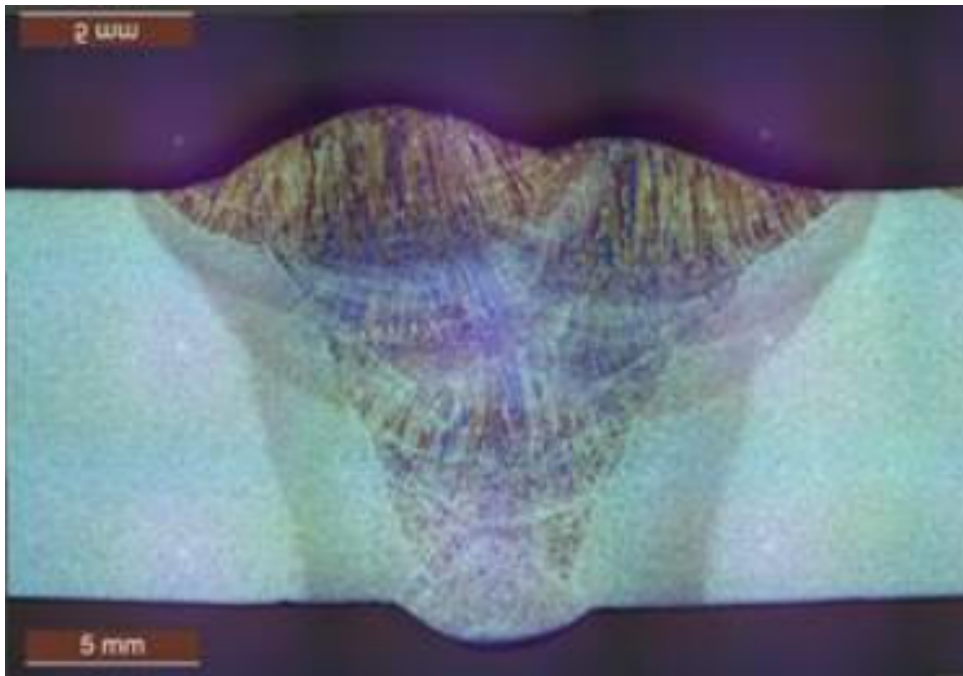Figure 4: Stress test sample next to ruler.

Figure 5: Image of the weld in the plate material. The shades from light to darkest show base material, Heat Affected Zone, and the weld material.
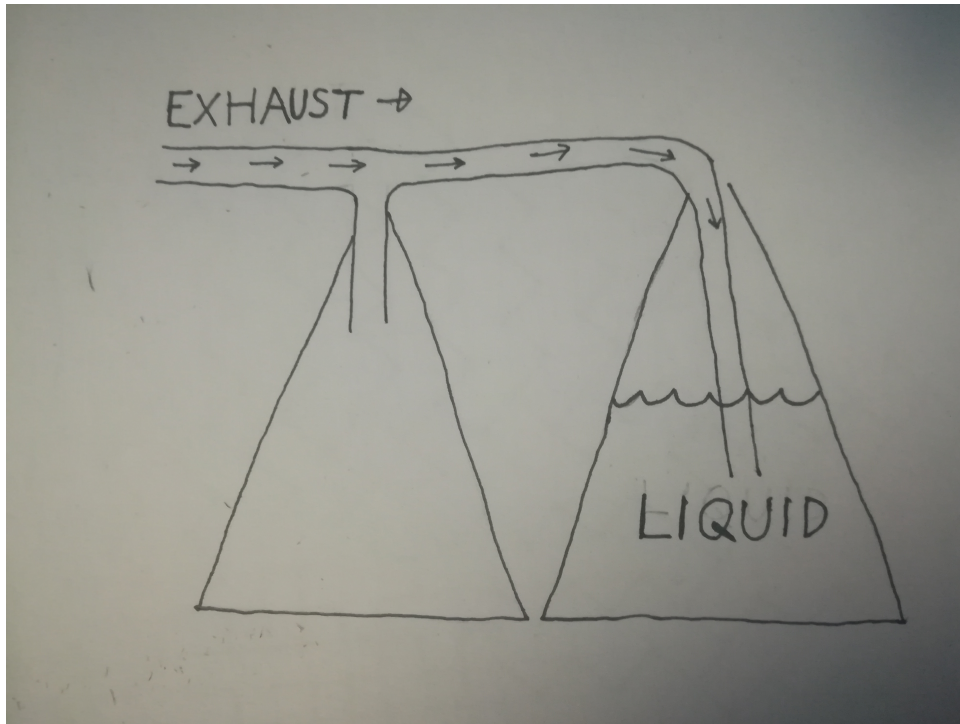
Figure 6: Sketch of the exhaust processing setup. Arrows indicate gas flow under normal operation, while any back flow is collected in the empty container.

until this no longer resulted in relaxation of the axis. The samples were also connected to the potentiostat, which would record the potential on the samples when not turned on. Fully mounted, the samples were submerged in the fluid before the autoclave was sealed save for the gas exhaust in the lid. Any fluid over the level of the exhaust outtake was flushed back into the container by sending N_2 gas into the autoclave until no more liquid came out of the exhaust.

During the rest of the test, the gas exhaust was funneled into the nearby fume hood, where it went into a container of liquid in order to give a qualitative measure of the rate of gas flow. In case of low pressure developing in the autoclave, there was an empty flask connected between the liquid container and the autoclave, which would collect any liquid instead of seeing it sucked into the autoclave, which would disturb the test conditions. The setup is sketched in Figure 6. N_2 was sent through the autoclave for at least 2 hours to evacuate the oxygen, followed by the test gas for another minimum 2 hours before starting the test run. The test gas during this stage was sent through at a rate producing a handful of bubbles per second, but without heavily disturbing the surface of the water in the control container.

During the gas infusion, the temperature was brought to $60\,°C$. After the infusion stage, the gas bubbling was reduced to a level of one bubble every 2-3 seconds, and the test was initiated with the loading units moving at a constant rate $1.8\,\mu m\,min^{-1}$, corresponding to a constant strain rate of $10^{-6}s^{-1}$ relative to a sample length of $30\,mm$. After both samples had undergone fracture, the autoclave was flushed with N_2 and permitted to cool for a couple of hours. The exhaust was then opened completely to

Figure 7: Slow Strain Rate samples of S235JR steel loaded into the Cormet prior to submersion in the MEA solution.

ensure there was no excess pressure inside the autoclave before opening. Samples were then extracted, and the used solution was tapped into a waste container. After extraction, samples were immediately washed off with acetone, distilled water, and ethanol, then dried and placed in a dessicator. An overview of each experiment is given in Table 3.

For the tests where H_2S was present in the autoclave, the procedure during set up and operation was altered to account for the toxicity of the gas, as well as the chemical absorption of H_2S in the MEA solution. The flask containing the H_2S mixtures was placed and secured inside the fume hood. A barometer was installed between the nozzle of the flask and the autoclave in order to keep track of the pressure provided from the flask. This was then compared to the pressure registered by the Cormet itself. In both H_2S trials (tests 5 and 7) gas was sent into the autoclave with the exhaust closed after flushing with N_2. The pressure was set to 1 bar in test 5, and 1.2 bar in test 7. When the autoclave's internal pressure stabilized as equal to the flask's output, the solution was taken to be saturated. An attempt was made at this point in test 5 to measure the concentration of H_2S in the solution using a hydrogen sulfide test kit from CHEMetrics. The indicator proved insoluble in the MEA, and so this was not attempted in test 7. With the solution saturated, a slow trickle of gas was permitted to pass through the exhaust to give room for replacement gas. The exhaust in these experiments was passed through a 10% NaOH solution, which chemically destroys most of the H_2S.

In Test 7, the flask containing 7.30% H_2S was in danger of running out after a few hours, and was swapped for the gas containing 4.83% H_2S. To maintain the same partial pressure of H_2S, the total pressure in the autoclave was increased to 1.8 bar at this point.

In test 5, the end of test procedure was carried out as normal due to the minuscule

9

Table 3: Summary of performed SSRT tests

Test	Samples	Test conditions
1	8 and 9	Distilled water with Pure N_2 Reference for samples without weld
2	10 and 11	30% MEA with Pure N_2 Reference for samples without weld
3	12 and 13	30% MEA with 10% CO_2, 10% O_2, 80% N_2 and cathodic protection $-1050\,\text{mV}$ vs. Ag|AgCl on samples. Interrupted by equipment failure
4	14 and 15	30% MEA with 10% CO_2, 10% O_2, 80% N_2 and cathodic protection $-1050\,\text{mV}$ vs. Ag|AgCl on samples. Samples without weld
5	16 and 17	30% MEA with 0.0001 bar H_2S, 0.1 bar CO_2, and 0.9 bar N_2 Samples without weld
6	18 and 19	air at ambient temperature Reference for samples without weld
7	20 and 21	30% MEA with 0.088 bar H_2S and 1.112 or 1.776 bar CO_2 Samples without weld
8	22 and 23	30% MEA with 10% CO_2, 10% O_2, 80% N_2 and cathodic protection $-1150\,\text{mV}$ vs. Ag|AgCl on samples. Samples without weld
9	1 and 2	30% MEA with 10% CO_2, 10% O_2, 80% N_2 and cathodic protection $-1150\,\text{mV}$ vs. Ag|AgCl on samples. Samples with weld
10	3 and 4	"CCX2" with 10% CO_2, 10% O_2, 80% N_2 Samples with weld
11	5 and 6	30% MEA with 10% CO_2, 10% O_2, 80% N_2 and cathodic protection $-1050\,\text{mV}$ vs. Ag|AgCl on samples. Samples with weld
12	24 and 25	30% MEA with 10% CO_2, 10% O_2, 80% N_2 Samples without weld
13	33 and 34	30% MEA with 10% CO_2, 10% O_2, 80% N_2 and cathodic protection $-1050\,\text{mV}$ vs. Ag|AgCl on samples. Preloaded samples with weld.
14	27 and 28	30% MEA with 10% CO_2, 10% O_2, 80% N_2 and cathodic protection $-1050\,\text{mV}$ vs. Ag|AgCl on samples. Preloaded samples without weld.
15	26 and 29	"CCX2" with 10% CO_2, 10% O_2, 80% N_2 Samples without weld
16	35 and 37	Air at ambient temperature Reference for samples with weld

amounts of H_2S in the test gas. In test 7, end of test procedure was carried out while wearing gas masks for safety. The test solution was pushed through a tube into a dedicated waste container inside the fume hood. This was accomplished by attaching the tube to the drain valve at the bottom of the autoclave, then sealing all other exits before pushing N_2 gas into the autoclave. Once this was accomplished, the autoclave was further flushed with N_2 gas for a couple of minutes before opening and extracting the samples.
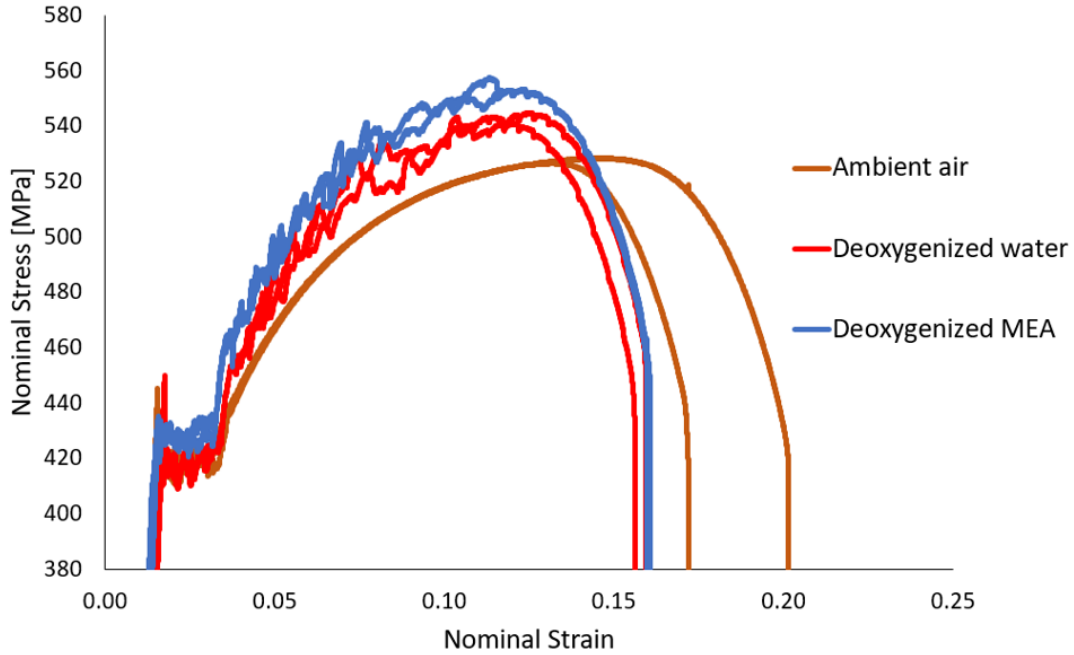
Figure 8: Stress-Strain curves for S235JR in tensile tests at strain rate $10^{-6}s^{-1}$. Comparison of reference tests in ambient air and aqueous environments saturated with N_2 at $60\,°C$.

4 Results

4.1 Homogeneous Samples

Figure 8 shows comparison between the three reference tests in ambient air and deoxygenized aqueous environments at $60\,°C$. The aqueous tests were recorded breaking earlier than the test in ambient air. There was very little difference between water and MEA.

Figure 9 shows testing in MEA saturated with 10% O_2, 10% CO_2, and 80% N_2 compared to the MEA reference. Very little difference was observed between the stress-strain relationships.

Figure 10 shows how the "CCX2" performs compared to the benchmark 30% MEA solution when saturated with 10% O_2, 10% CO_2, and 80% N_2.

Figure 11 shows that all samples that were cathodically protected fractured before the samples that were not. The samples held at $-1150\,mV$ lie between those held at $-1050\,mV$, while the preloaded samples have very low variance.

Figure 12 shows the H_2S tests compared to the MEA reference. Compared to the reference test, introducing H_2S to the system showed minimal effect, and the samples exposed to high amounts of H_2S took slightly longer to fracture than the reference. During the high H_2S concentration test, 20 bar of the gas mixture of 7.30% H_2S and 92.70% CO_2 was consumed from the $10\,L$ flask before the test solution began to reach saturation.
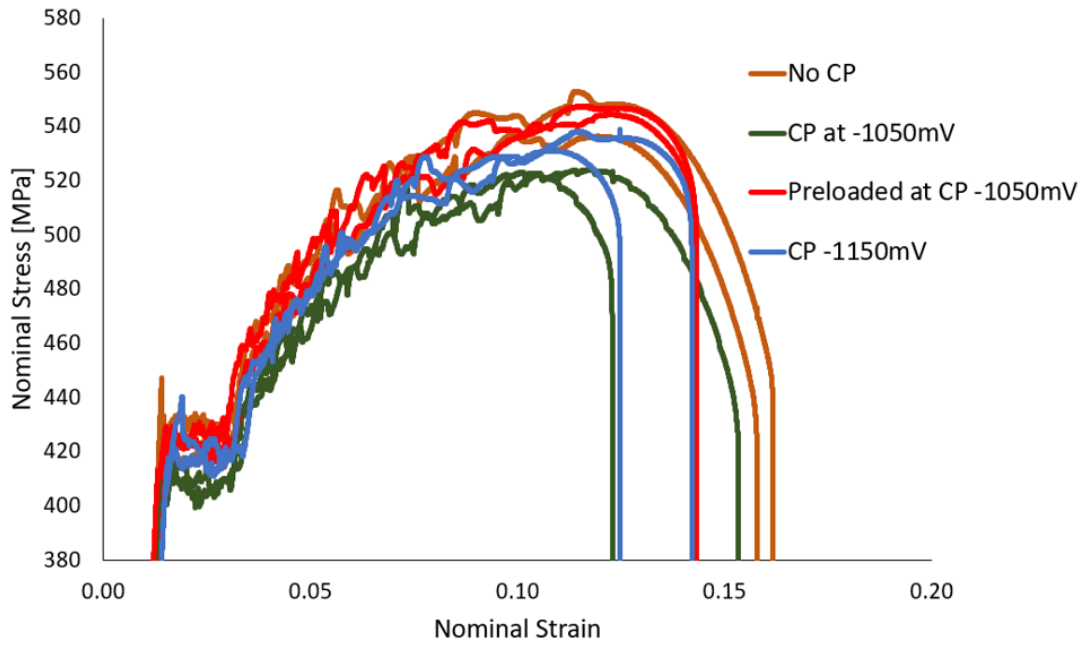
12
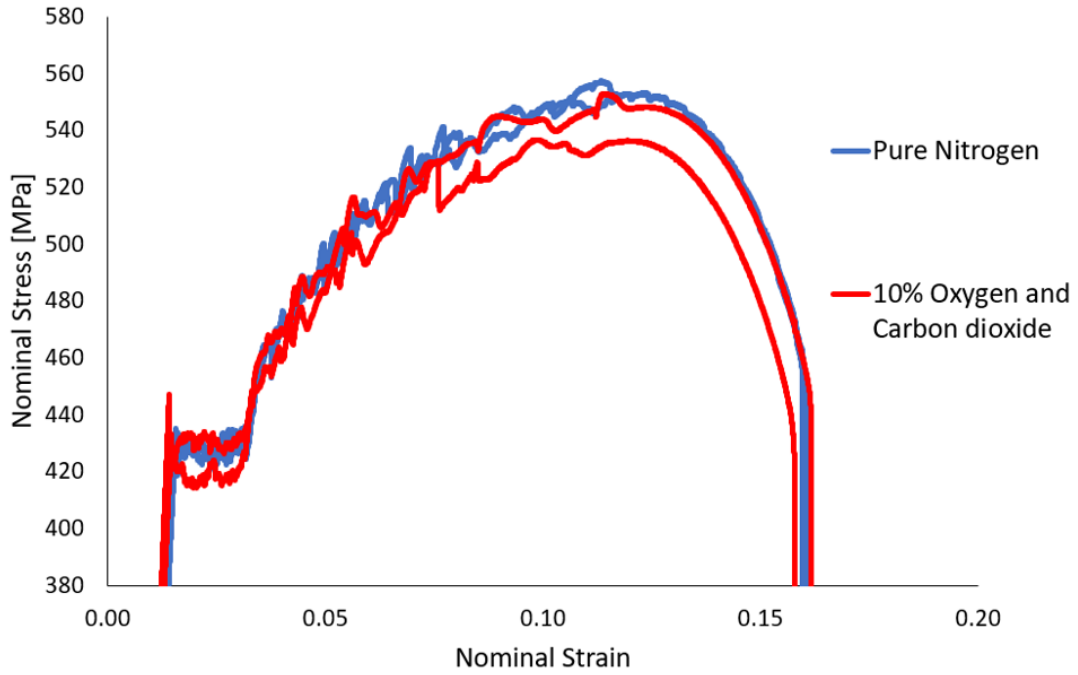
Figure 9: Stress-Strain curves for S235JR in tensile tests at strain rate $10^{-6}\mathrm{s}^{-1}$ in 30% MEA at 60 °C saturated with gas mixture of 10% O_2, 10% CO_2 and 80% N_2 compared to reference saturated with pure N_2.
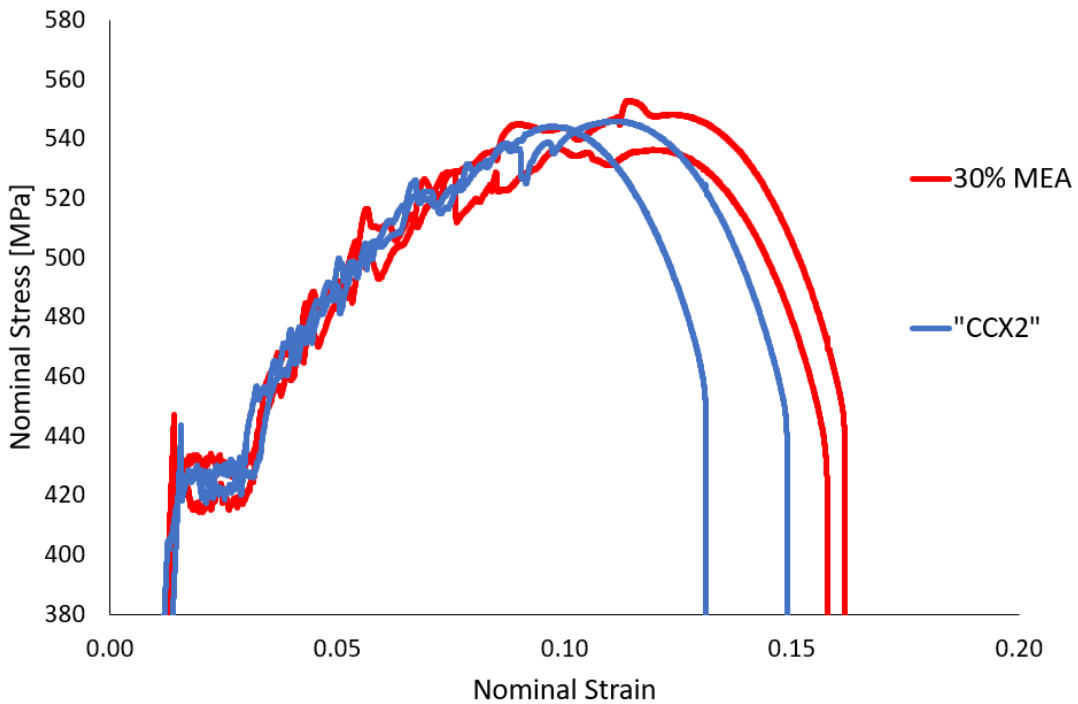
Figure 10: Stress-Strain curves for S235JR in tensile tests at strain rate $10^{-6}\mathrm{s}^{-1}$ in 30% MEA and "CCX2" at 60 °C, each saturated with gas mixture of 10% O_2, 10% CO_2 and 80% N_2.

Figure 11: Stress-Strain curves for S235JR in tensile tests at strain rate $10^{-6}s^{-1}$ in 30% MEA at 60 °C saturated with gas mixture of 10% O_2, 10% CO_2 and 80% N_2. Two levels of impressed potential cathodic protection were used. Preloaded samples were held at the protection potential for 11 days before the test.
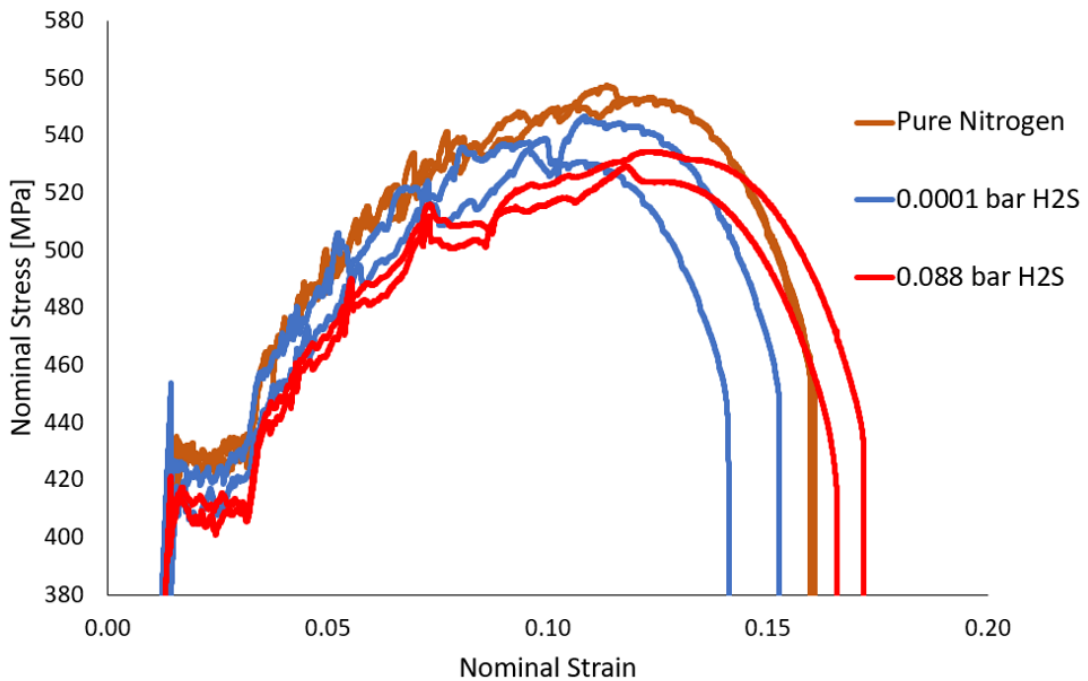
Figure 12: Stress-Strain curves for S235JR in tensile tests at strain rate $10^{-6}s^{-1}$ in 30% MEA at 60 °C with varying partial pressure of H_2S

14
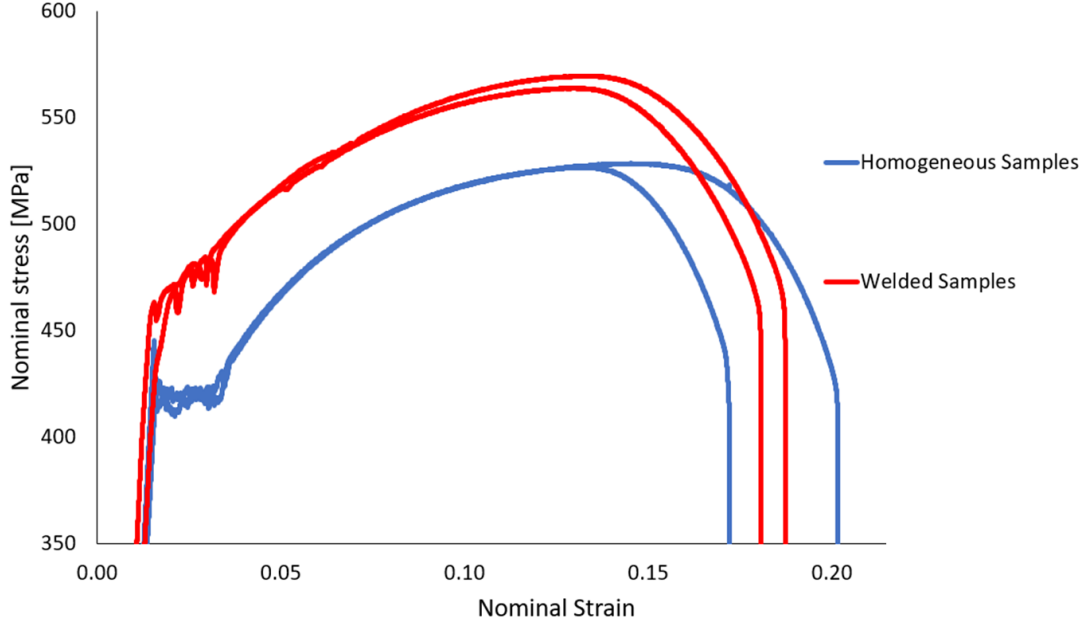
Figure 13: Stress-Strain curves for S235JR in tensile tests at strain rate $10^{-6}\mathrm{s}^{-1}$ in ambient air with and without included weld in the samples. Strain increments of the welded samples above $400\,\mathrm{MPa}$ are stretched x1.35.

4.2 Welded samples

4.2.1 Strain estimation

When performing the slow strain rate tests on the welded samples they were found to generally last shorter than the homogeneous samples, but, with one exception, showed no indication of a brittle fracture. Furthermore, the samples always fractured near one end or the other of the sample, never in the weld. Knowing that the weld material is stronger than the base material, it was assumed that the effective sample length was shorter for the welded samples. Thus, strain would not be possible to calculate as for the homogeneous samples, making comparison of the two difficult. The following assumptions were made in order to obtain an estimate of the strain:

1. The elastic behavior of the welded samples is identical to that of the homogeneous samples.

2. The weld constitutes a band of uniform thickness $7.78\,\mathrm{mm}$ in the middle of the sample.

3. The weld undergoes no plastic deformation.

Following these assumptions, a cut-off point for the elastic region was chosen at $400\,\mathrm{MPa}$. Above this stress value, each strain increment in the recorded data assuming sample length $30\,\mathrm{mm}$ was multiplied by $\frac{30}{30-7.78} = 1.35$. A comparison of reference tests done in air at ambient temperature for the welded and homogeneous is given in Figure 13.
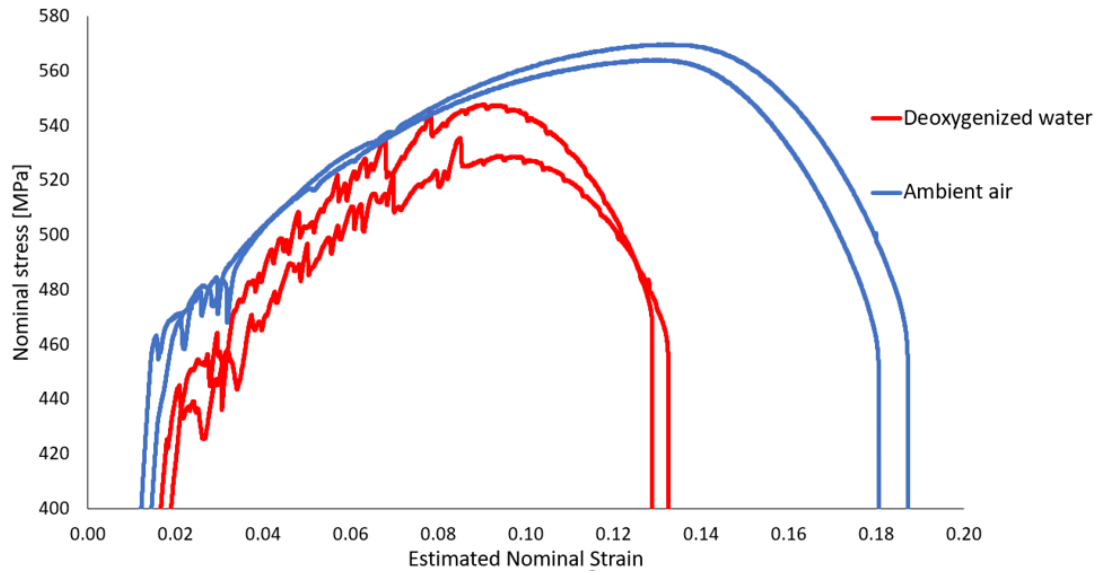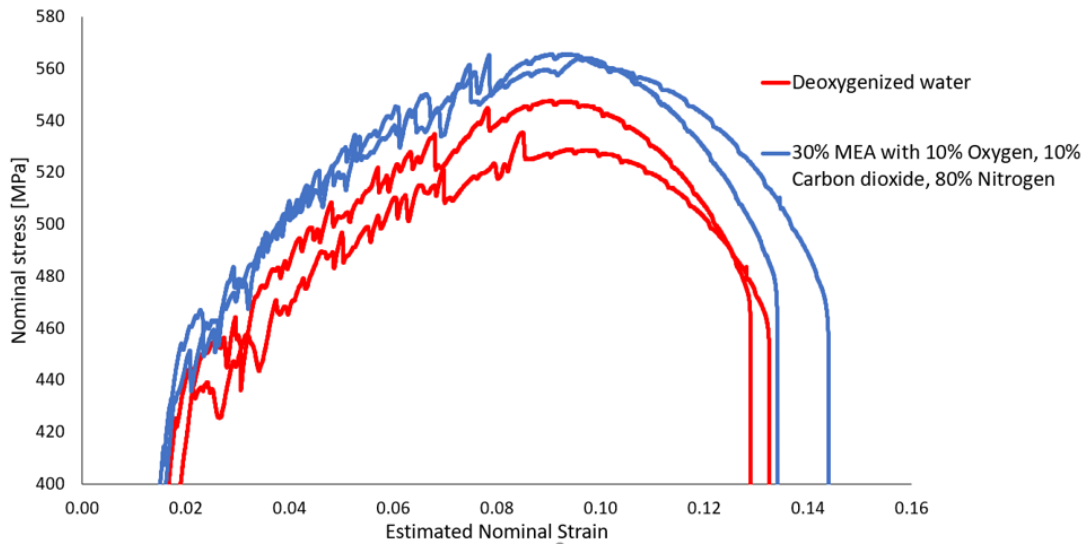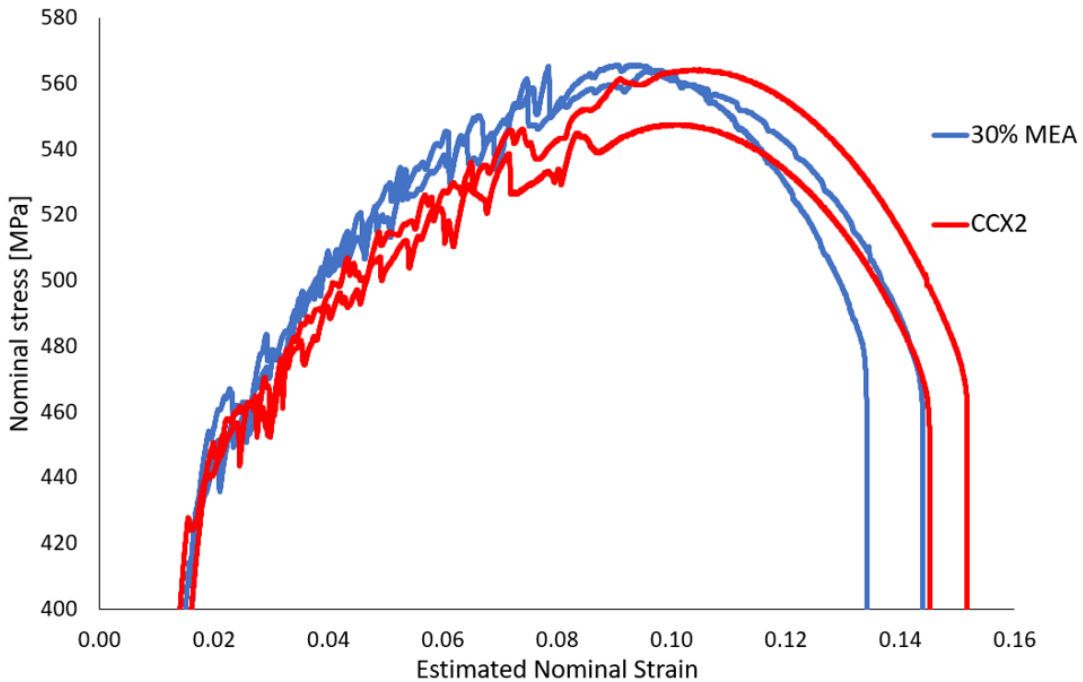
15

Figure 14: Stress-Strain curves for S235JR with included weld in tensile tests at strain rate 10^{-6}s^{-1} relative to full sample length. Comparison of reference test in ambient air and distilled H_2O saturated with N_2 at $60\,°C$.

As long as the assumption that the weld undergoes no plastic deformation holds, the stress-strain curves for the welded samples should be comparable to that of the homogeneous samples in the absence of an environmental effect. Figure 13 indicates that under identical test conditions, the strain estimation described above gives a close match to the expected results. As such, the estimation is used for presenting stress-strain relationships of the performed tests.

4.2.2 Stress-Strain relationships of welded samples

Figure 14 shows comparison between the reference test in ambient air and data for de-oxygenized water at $60\,°C$. The test in water was carried out earlier as part of the master specialization project of the author, Sigurd Gaut. The test procedures were the same, and the data presented here is processed directly from the raw data. The aqueous tests were recorded breaking earlier than the test in ambient air. Due to time constraints, no reference test in 30% MEA was carried out for the welded samples. The aqueous environment was much harsher on the samples than ambient air

Figure 15 shows testing in MEA saturated with 10% O_2, 10% CO_2, and 80% N_2 compared to the water reference. The MEA test was done as part of the aforementioned master project the H_2O reference was lifted from, and follows the same treatment. Very little difference was observed between the stress-strain relationships.

Figure 16 shows how the welded samples perform in the "CCX2" mixture compared to the benchmark 30% MEA solution when saturated with 10% O_2, 10% CO_2, and 80% N_2. Very little difference was observed.

Figure 17 shows the samples that were cathodically protected compared to each other. The samples held at $-1150\,\text{mV}$ lie between those held at $-1050\,\text{mV}$, while the preloaded samples have low variance compared to the other tests, and also fractured somewhat later
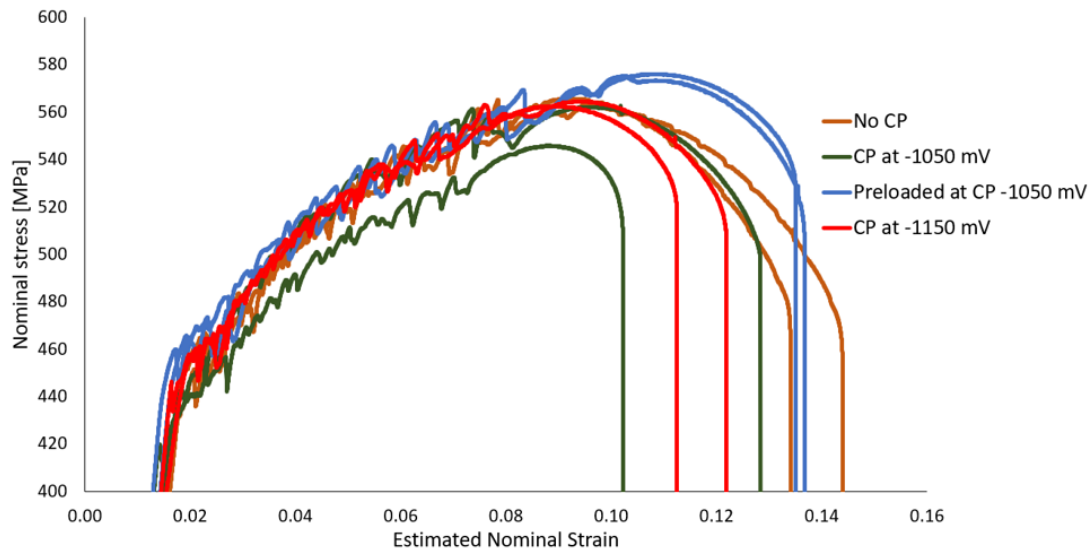
16

Figure 15: Stress-Strain curves for S235JR with included weld in tensile tests at strain rate 10^{-6}s^{-1} relative to full sample length. Testing in 30% MEA at $60\,^{\circ}\text{C}$ saturated with gas mixture of 10% O_2, 10% CO_2 and 80% N_2 is compared to reference in H_2O saturated with pure N_2.

Figure 16: Stress-Strain curves for S235JR with included weld in tensile tests at strain rate 10^{-6}s^{-1} relative to full sample length. Comparison of 30% MEA and "CCX2" at $60\,^{\circ}\text{C}$, each saturated with gas mixture of 10% O_2, 10% CO_2 and 80% N_2.

17

Figure 17: Stress-Strain curves for S235JR with included weld in tensile tests at strain rate 10^{-6}s^{-1} relative to full sample length in 30% MEA at 60 °C saturated with gas mixture of 10% O_2, 10% CO_2 and 80% N_2. Two levels of impressed potential cathodic protection were used. Preloaded samples were held at the protection potential for 8 days before the test.

than the samples that were not preloaded. The unprotected samples also lasted longer than the samples that were not preloaded. One of the samples held at $-1050\,\text{mV}$ had a significantly shorter lifetime than any other sample, and also showed less signs of necking. The two samples from this test were imaged in the SEM for further analysis.

4.2.3 SEM images of Samples 5 and 6

The samples from the test on welded samples held at impressed potential $-1050\,\text{mV}$ were imaged in the SEM. This was done because sample 6 had showed significantly shorter lifetime than any other sample. Figure 18 shows images of the fracture surfaces on sample 5. The surface is uneven, and exhibits multiple dimples throughout.
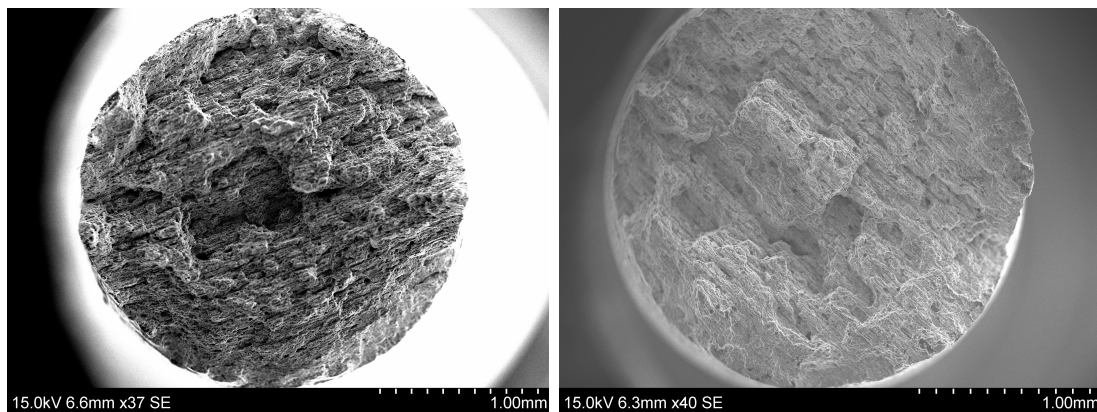
(a) Short end   (b) Long end

Figure 18: Overview of the fracture surfaces of Sample 5

18

Figure 19 a) and b) shows images of the fracture surfaces on sample 6. This fracture surface is quite flat with the exception of a notable bulge near the top of the overview images. The bulge exhibits obvious dimples, while the flat areas seem not to on the overview. A closer look at the flat area near the center of the fracture surface is shown in Figure 19 c). This shows some signs of dimples, though much less so than in sample 5.
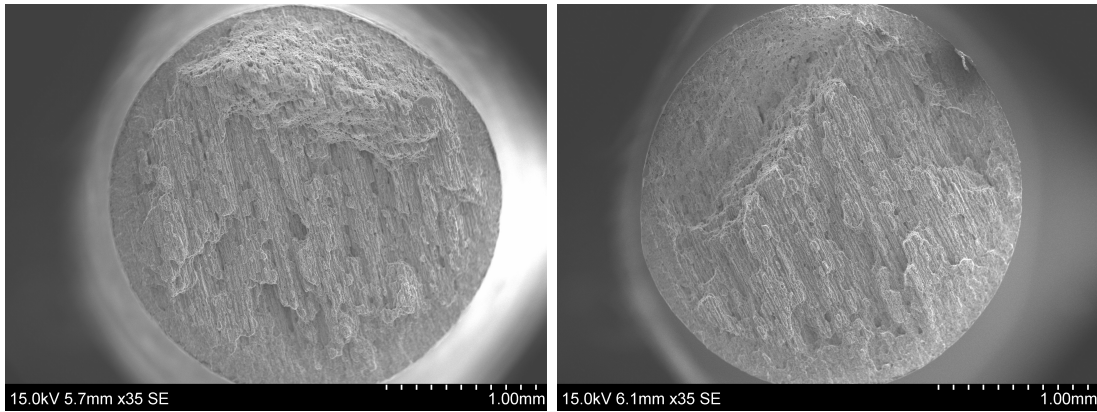
(a) Short end

(b) Long end
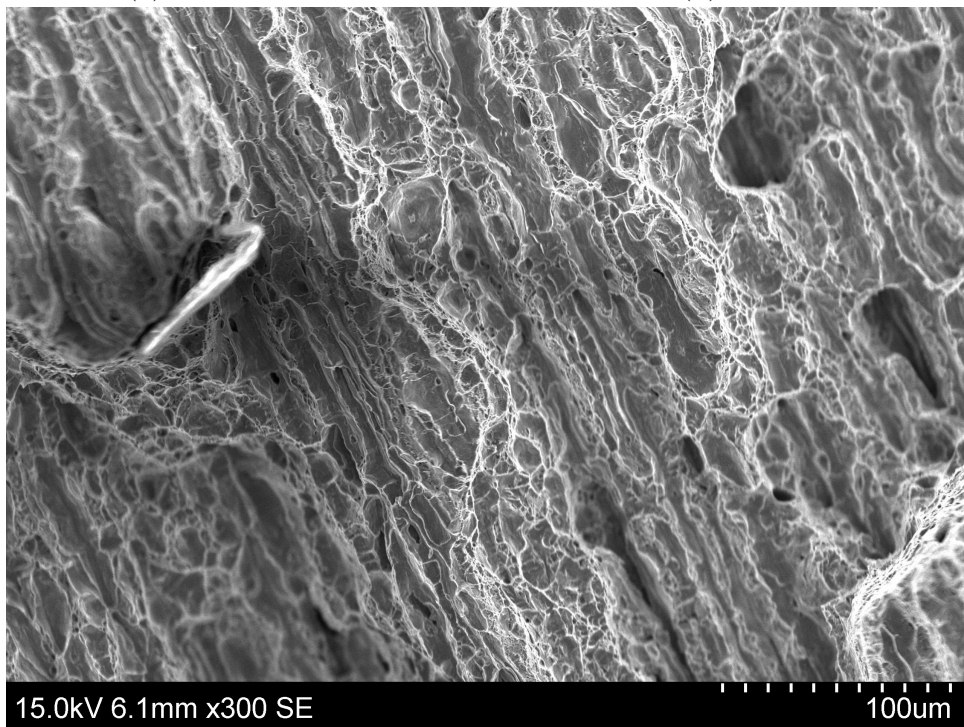
(c) A closer look at the long end

Figure 19: Fracture surfaces of Sample 6

5 Discussion

Most of the experiments show a significant degree of experimental variation between the samples undergoing the same treatment. This obviously limits the ability to draw trends from the data. Nonetheless, certain trends may be hinted at despite the inability to draw definite conclusions without additional data. Of note in this regard is that the experiments which showed the least variation were first, the ones where pure N_2 was used for the atmosphere, and second, the ones where samples held at a cathodic protection potential were preloaded. This could be a coincidence, but these environments are also the ones where the least degree of corrosion reactions are expected. It should be noted while this trend was seen for both homogeneous and welded samples, the experiments with cathodic protection where the samples were not preloaded showed significant variation. The preloaded samples might have become more stable than the ones that were not, and in fact seemed to have higher UTS and strain before fracture, as can be seen in Figures 11 and 17. This is certainly evidence against Hydrogen Induced Cracking as a likely mechanism in this system.

The welded samples have an additional layer of interpretation. As discussed in Section 4.2.1, the stress-strain curves could not be calculated as straight-forward as for the homogeneous samples due to the overmatch weld. Based on the ambient air reference tests, a stretching factor of 1.35 on the plastic deformation seems to give a good estimation of strain. This is only an estimation, however, and relies on assumptions that have not been tested within the scope of this work. The first assumption, that elastic behavior is identical to the homogeneous material appears valid, evidenced by the elastic un-stretched segment of the stress-strain curve overlapping closely for both the homogeneous and welded samples. The second assumption, regarding the weld thickness, simplifies the reality of a weld which is both of uneven thickness within a given sample, and not guaranteed to be identical in each sample. Finally, the assumption that the weld undergoes no plastic deformation is based on the knowledge that the weld is supposed to have higher strength than the base material. An extensometer could have been used to measure the weld deformation exactly, but this equipment was not available. Supporting the assumption, all of the welded samples experienced fracture near one end of the sample regions, far away from the weld.

A significant difference between the welded samples and the homogeneous samples is that the former do not display the Lüders plateau behavior. This might suggest that the dislocation "pinning" mechanism is not observed in these samples. Alternatively, this could imply the weld has left residual stress concentrations, such that instead of the Lüders plateau, the material smoothly transitions into strain hardening.

The welded samples also generally exhibit noticeably higher UTS than the homogeneous samples. Assuming the weld doesn't experience any deformation, this can be attributed to higher strain rate. This occurs because while the weld material does not contribute to the effective sample length, the loading units were moving at the same rate for all the samples, welded or not. Thus the S235 steel has been shown to be strain rate sensitive[12].

None of the stress-strain curves recorded show clear signs of brittle fracture. One welded sample, number 6, showed tendencies of brittle behavior when exposed to an impressed potential of $-1050\,\mathrm{mV}$ vs Ag|AgCl. The SEM images taken of this fracture

surface shows little evidence of dimpling except for a small area, suggesting a less ductile or brittle fracture. The fracture was almost cleanly orthogonal, unlike the other fractures. A closer look did reveal tendencies of what might be dimples elsewhere in the fracture surface as well. There is not enough evidence to draw definite conclusions from this, but one might tenuously state that the combination of a weld, the gas mixture of 80% N_2 10% CO_2, 10% O_2 bubbled through 30% MEA at atmospheric pressure, a cathodic protection potential and $60\,°C$ might result in embrittling tendencies in the material. Further examination of these conditions is recommended.

When comparing the performance of the "CCX2" mixture to the 30% MEA, it is not possible to claim a significant difference was observed. Even so, it should be noted that for the homogeneous samples, the MEA test ran longer, while for the welded samples, the "CCX2" test ran longer than the MEA test. Neither of these variations can securely be said to be significant, however, and from the limited data available the two amine solutions appear to have equally non-adverse effects on the steel. The MEA test for the welded case was from an older test.

Testing in environments with H_2S was only carried out on homogeneous samples due to lack of gas. As is seen from Figure 12 neither the low H_2S nor high H_2S environments were significantly different from the reference with a pure N_2 atmosphere. Interestingly, when H_2S is present, the higher concentration, saturated at 0.088 bar partial pressure, seems to have granted the samples a longer lifetime than the low concentration. If the differences that are observed were to be greatly exaggerated, the Ultimate Tensile Strength and yield strength show a very slight deterioration with increasing H_2S.

Finally, the observed absorption of CO_2 and H_2S bears commenting on. The experimental setup was not designed to measure this, but in Test 7, it was observed that approximately $200\,L$ of gas containing 7.30% H_2S and 92.7% CO_2 was absorbed in the solution of 30% MEA. This corresponds to around $364\,g$ CO_2 and $11.7\,g$ H_2S. The autoclave has an internal volume of $3.5\,L$, so these values correspond to approximately $1\,L$ of MEA.

6 Conclusion

S235JR steel seems to maintain ductile behavior in the amine environments of a carbon capture system at $60\,°C$. Neither introduction of cathodic protection, dissolved and absorbed H_2S or CO_2, nor an included weld in the tensile samples resulted in a clearly brittle fracture. However, indications of a partially brittle nature was found in the failure of one sample with an included weld held at cathodic protection potential $-1050\,mV$ vs. Ag|AgCl, and more investigation is needed in this area in order to draw a definite conclusion regarding potential HIC or SCC vulnerability in the steel. Finally, in the conducted tests, the "CCX2" mixture of amines performed comparably to the 30% MEA solution with regard to material properties.

References

[1] J. G. Speight, "Stress-corrosion cracking," in *Rules of Thumb for Petroleum Engineers*. 2017. [Online]. Available: `https://app.knovel.com/hotlink/khtml/id:kt011HVBHB/rules-thumb-petroleum/stress-corrosion-cracking` (visited on 01/06/2019).

[2] Y. F. Cheng, "Fundamentals of stress corrosion cracking," in *Stress Corrosion Cracking of Pipelines*. John Wiley & Sons Incorporated, 2013, pp. 7–42. [Online]. Available: `https://ebookcentral.proquest.com/lib/ntnu/detail.action?docID=1117022` (visited on 01/04/2019).

[3] M. S. DuPart, T. R. Bacon, and D. J. Edwards, "Understanding corrosion in alkanolamine gas treating plants," *Hydrocarbon Processing - HYDROCARB PROCESS*, vol. 72, pp. 75–80, Apr. 1993.

[4] E. B. of OGST, "Did you say the multiple facets of the problems encountered by the C=2 post-combustion capture?" *Oil & Gas Science and Technology*, vol. 69, no. 5, pp. 773–783, 2014. DOI: `10.2516/ogst/2014036`.

[5] "Corrosion in CO_2 post-combustion capture with alkanolamines - a review," English, *Oil & Gas Science and Technology*, vol. 69, no. 5, pp. 915–929, Nov. 2013, Copyright - Copyright IFP Energies Nouvelles 2013. [Online]. Available: `https://ogst.ifpenergiesnouvelles.fr/articles/ogst/abs/2014/05/ogst130037/ogst130037.html`.

[6] Y. Tomoe and M. Shimizu, "Corrosivity difference among primary alkanolamines when loaded with CO_2," *Journal of the japanese association for petroleum technology*, vol. 66, no. 4, Jul. 2001.

[7] "Survey updates amine stress corrosion cracking data," English, *Oil & Gas Journal*, vol. 90, no. 2, p. 42, Jan. 1992, Copyright - Copyright PennWell Publishing Company Jan 13, 1992; Last updated - 2012-06-06; CODEN - OIGJAV. [Online]. Available: `https://search.proquest.com/docview/274292206?accountid=12870`.

[8] E. Steel and A. Grades/number. (). S235jr (1.0038(dubl)), [Online]. Available: `http://www.steelnumber.com/en/steel_composition_eu.php?name_id=4` (visited on 01/02/2019).

[9] Ovako. (). S235jr material datasheet, [Online]. Available: `https://steelnavigator.ovako.com/steel-grades/s235/` (visited on 06/30/2019).

[10] W. D. C. Jr. and D. G. Rethwisch, *Materials Science and Engineering*, 9th ed. John Wiley & Sons Incorporated, 2015.

[11] J. Belotteau, C. Berdin, S. Forest, A. Parrot, and C. Prioul, "Mechanical behavior modeling in the presence of strain aging," in *Fracture of nano and engineering materials and structures, ECF 16*, E. Gdoutos, Ed., Alexandroupolis, Greece: Springer, Jul. 2006, 8 p. [Online]. Available: `https://hal.archives-ouvertes.fr/hal-00832996`.

[12] P. Larour, "Strain rate sensitivity of automotive sheet steels: Influence of plastic strain, strain rate, temperature, microsturcture, bake-hardening and pre-strain," Apr. 2010.

Appendices

A   Figures

Figures comparing the homogeneous samples to the welded samples case by case for the configurations where data exists for both samples with and without the included weld are shown in Figures 20-26
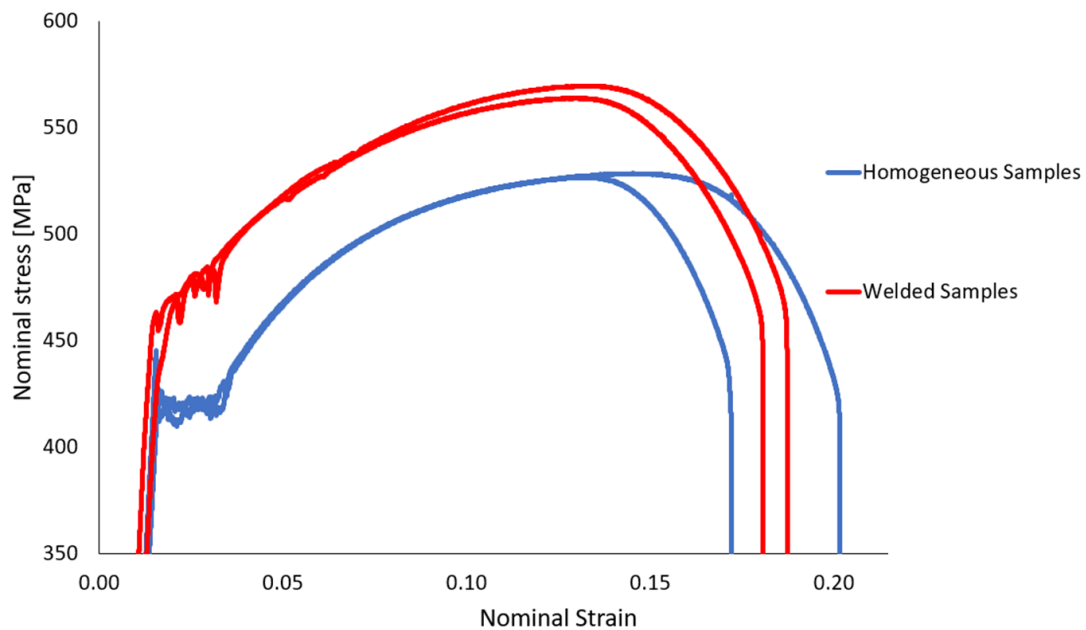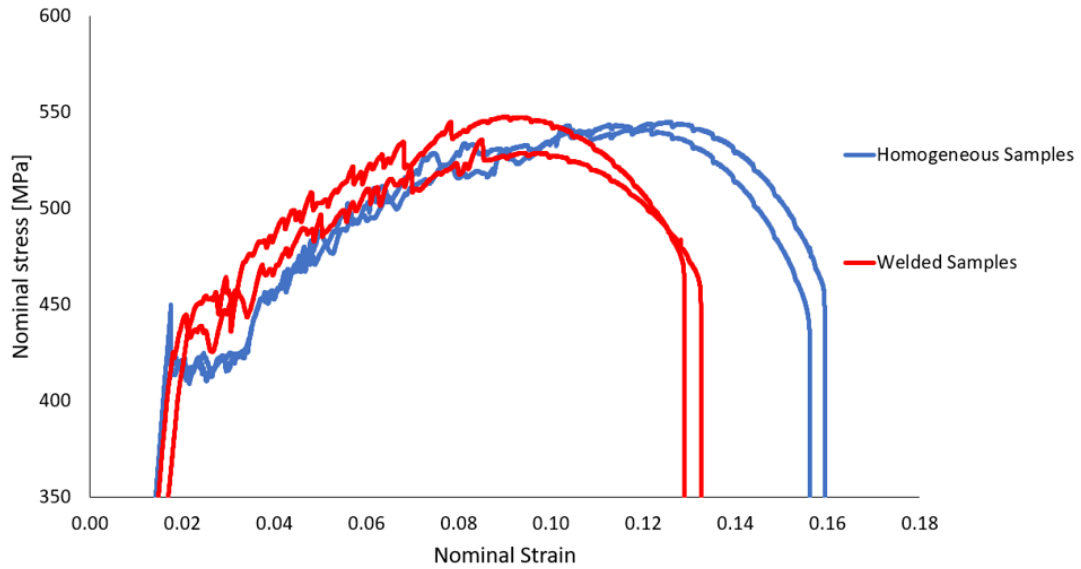

Figure 20: Comparison of samples in air at ambient temperature. Welded samples are assumed to experience all deformation in the base material, and the weld takes up about 26% of the sample length. Thus all straining of the welded samples beyond 400 MPa is multiplied by 1.35 to account for this.

Sample number	Weld	thickness [mm]	Used in test
1	yes	3.15	9
2	yes	3.14	9
3	yes	3.15	10
4	yes	3.16	10
5	yes	3.16	11
6	yes	3.17	11
8	no	3.14	1
9	no	3.13	1
10	no	3.11	2
11	no	3.13	2
12	no	3.11	3
13	no	3.11	3
14	no	3.18	4
15	no	3.17	4
16	no	3.13	5
17	no	3.11	5
18	no	3.16	6
19	no	3.18	6
20	no	3.18	7
21	no	3.19	7
22	no	3.17	8
23	no	3.17	8
24	no	3.12	12
25	no	3.15	12
26	no	3.15	15
27	no	3.14	14
28	no	3.13	14
29	no	3.12	15
33	no	3.11	13
34	no	3.12	13
35	yes	3.13	16
37	yes	3.11	16

Table 4: Overview of samples used in the experiments. Sample number corresponds to the physical labeling of the samples, thickness indicates minimal thickness.

Figure 21: Comparison of samples in distilled H_2O saturated with N_2. Welded samples are assumed to experience all deformation in the base material, and the weld takes up about 26% of the sample length. Thus all straining of the welded samples beyond $400\,\mathrm{MPa}$ is multiplied by 1.35 to account for this.
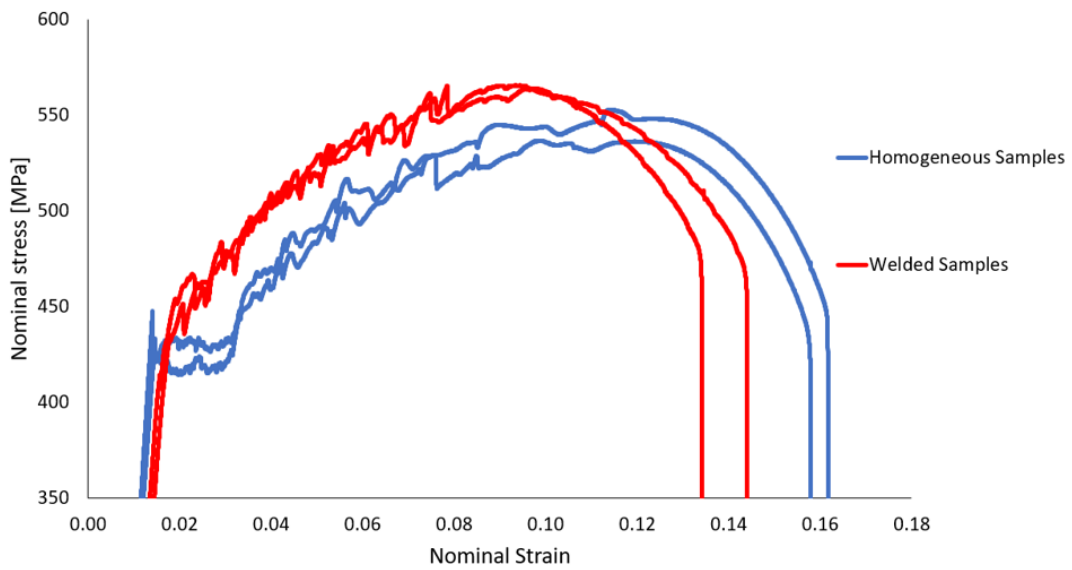
Figure 22: Comparison of samples in 30% MEA saturated with 10% O_2, 10% CO_2, and 80% N_2. Welded samples are assumed to experience all deformation in the base material, and the weld takes up about 26% of the sample length. Thus all straining of the welded samples beyond $400\,\mathrm{MPa}$ is multiplied by 1.35 to account for this.

25
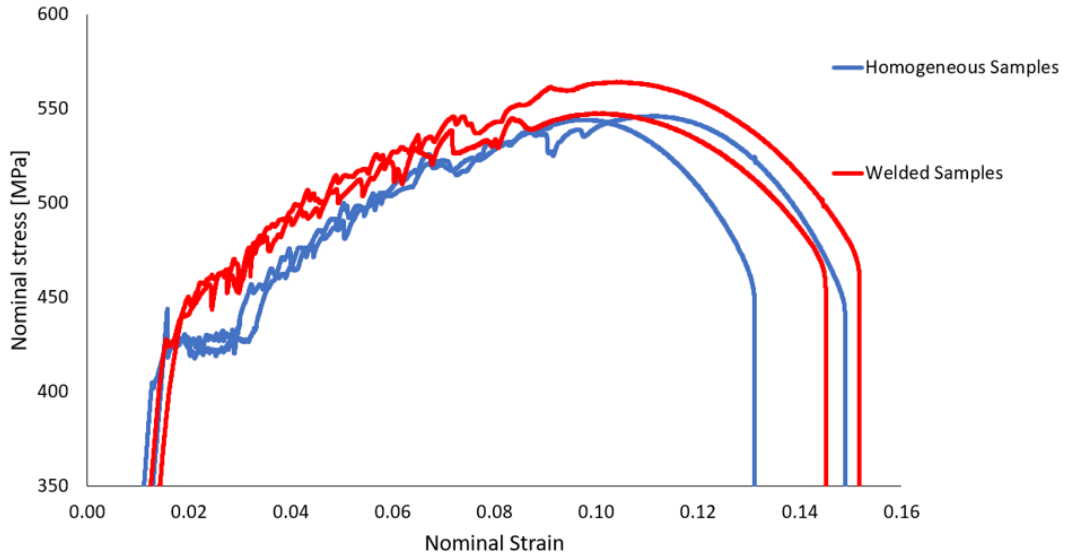
Figure 23: Comparison of samples in "CCX2" saturated with 10% O_2, 10% CO_2, and 80% N_2. Welded samples are assumed to experience all deformation in the base material, and the weld takes up about 26% of the sample length. Thus all straining of the welded samples beyond 400 MPa is multiplied by 1.35 to account for this.
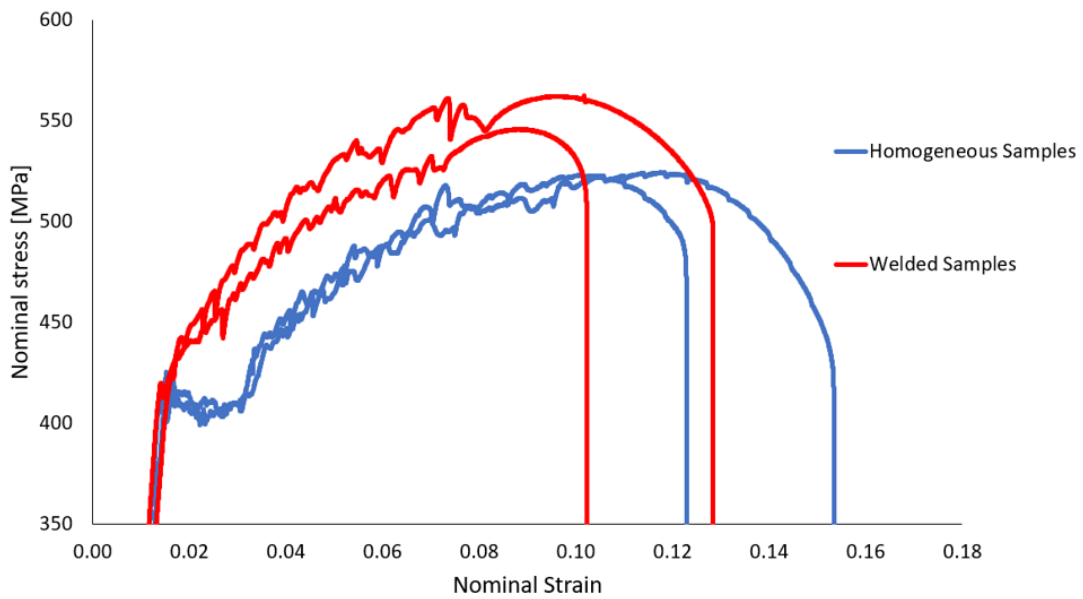
Figure 24: Comparison of samples in 30% MEA saturated with 10% O_2, 10% CO_2, and 80% N_2 while at an impressed potential -1050 mV vs. Ag|AgCl. Welded samples are assumed to experience all deformation in the base material, and the weld takes up about 26% of the sample length. Thus all straining of the welded samples beyond 400 MPa is multiplied by 1.35 to account for this.

26
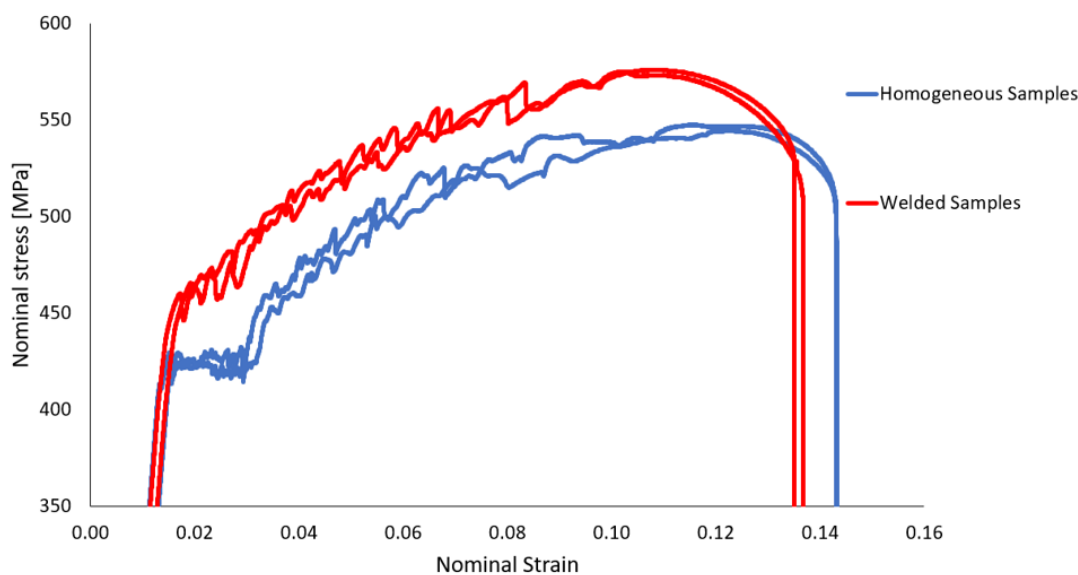
Figure 25: Comparison of samples in 30% MEA saturated with 10% O_2, 10% CO_2, and 80% N_2 while at an impressed potential $-1050\,\text{mV}$ vs. Ag|AgCl. Welded samples are assumed to experience all deformation in the base material, and the weld takes up about 26% of the sample length. Thus all straining of the welded samples beyond $400\,\text{MPa}$ is multiplied by 1.35 to account for this. Samples were held at the protection potential for several days before the test.
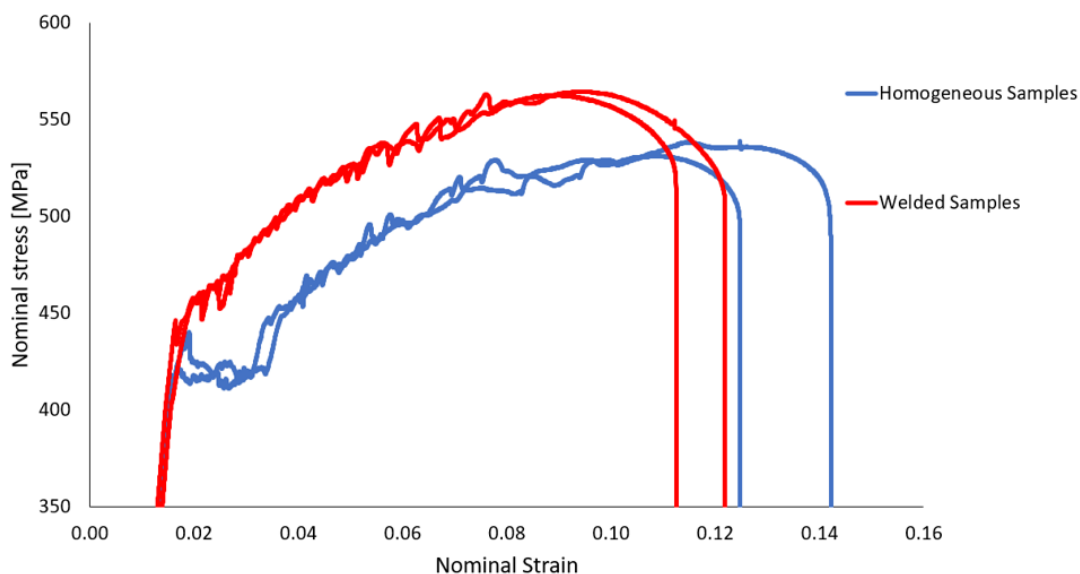
Figure 26: Comparison of samples in 30% MEA saturated with 10% O_2, 10% CO_2, and 80% N_2 while at an impressed potential $-1150\,\text{mV}$ vs. Ag|AgCl. Welded samples are assumed to experience all deformation in the base material, and the weld takes up about 26% of the sample length. Thus all straining of the welded samples beyond $400\,\text{MPa}$ is multiplied by 1.35 to account for this.

B   Gas Certificates

Figure 27: Certificate for gas mixture with low H$_2$S content.

PRAXAIR
Making our planet more productive

Sertifikat

Kunde: SINTEF Materialer og Kjemi	Sertifikat nr.: 78080272-01-K-711485	Flaske vannvolum (l): 10	Flaskenummer: K-711485
Kunde referanse: 551579 Ann-Karin Kvernbråten	Anbefalt trykkregulator: Ultraserien (SS)	Flaskeventilgjenger: DIN 477 No. 6	Fylletrykk v/20°C (bar g): 29,8

Komponenter	Bestilt sammensetning mol %	Sertifisert sammensetning mol %	Usikkerhet % relativ
H2S CO2	7,34 Rest	7,30 Rest	2

100 % LEL i luft (mol %):	Konfidens intervall: 95 % (k=2)	Kvalitetsklasse: 2	Kondensasjonstemp. ved fylletrykk (°C) 0	Stabilitetstid (måneder): 12
Laveste anbefalte brukstrykk (bar g): 3,0	Anbefalt lager og brukstemp. (°C) 20	Spesielle opplysninger:		
For sikkerhetsdatablad se www.praxair.no		Ved mistanke om utkondensering må flasken lagres horisontalt ved romtemperatur i 14 dager, eller rulles horisontalt i 8 timer ved ≥ 60 omdreininger/min før bruk.		

Vi er sertifisert iht. ISO 9001. Alle våre blandinger er sporbare til masse ved bruk av ISO 6142 eller ved sammenlignings-analyser mot standarder produsert ved bruk av ISO 6142. Sertifikat er utarbeidet iht. ISO 6141

Rjukan 19/2 - 2019 Tor Morten Hammer
(Produksjonssted) (Dato) (Ansvarlig)

Praxair Norge AS Fnr./Reg.No. 945 772 042

Postadr.
P.O.Box 23, Haugenstua
N-0915 OSLO

Telefon
+47 04 27 7

Telefax:
+47 24 15 64 29

Figure 28: Certificate for gas mixture with high H$_2$S content.

Figure 29: Certificate for gas mixture replacing the high H$_2$S content.